CERN-ACC-NOTE-2020-0049

September 2020

MD 3603: Dynamic Aperture with uncorrected dipole b_3

M. Hofer, F. Carlier, J. Dilly, E. Fol, A. Garcia-Tabares, E. H. Maclean, L. Malina, T. H. B. Persson, J. Coello de Portugal, M. Solfaroli Camillocci, R. Tomás, and A. Wegscheider
CERN, CH-1211 Geneva, Switzerland

Keywords: LHC MD, sextupole correction, forced Dynamic Aperture, free Dynamic Aperture

Summary

The hadron collider options currently investigated as part of the FCC study rely on the use of dipoles with a field strength of 16 T or above in order to achieve the targeted collision energy. From simulations of the current design of these dipoles, a systematic sextupole component of up to factor 10 larger than in the LHC dipoles could be present in these magnets. A similar systematic mispowering of the corrector circuits as is assumed in the LHC may thus have a significantly larger impact on the dynamic aperture and in turn potentially also on the operational performance. During this MD, the dynamic aperture in the presence of large sextupole fields in the LHC at injection energy was measured. By deliberately mispowering the sextupole spool pieces attached to each dipole, a large systematic b_3 component is generated and the subsequent change in chromaticity is corrected by the chromaticity sextupoles. Using both the aperture kicker and the AC-dipole as exciters, free and forced dynamic aperture as well as amplitude detuning were measured. Additional linear optics measurements provide insight into the contributions to coupling from the sextupole spool pieces.

Contents

1 Introduction

In the LHC as well as in other colliders using superconducting magnets, the correction of the systematic sextupole component of the main dipoles is critical both in terms of operation and dynamic aperture. This systematic field harmonic stems both from static contributions such as the coil geometry and persistent currents in the conductor as well as dynamic contributions from current redistributions in the superconducting cables leading to a change of the allowed harmonics such as the sextupole component at static current called decay. Once the ramping of the current starts, another dynamic change is observed, where the sextupole component changes back to the value before the decay, an effect which is called snap-back. Due to the large amount of dipoles, the integrated sextupole contribution would, if uncorrected, lead to a large chromaticity. Though easily correctable with chromaticity sextupoles and a feedforward system, the presence of this strong sextupole fields in turn also drives multiple resonances as well as leads to the generation of higher order chromaticity and amplitude detuning. In the LHC, a local correction provided by sextupole spool pieces (MCS) attached to each dipole [1] together with a dipole sorting strategy [2] was implemented. In addition, a large effort was put into assessing the field quality of the main dipoles, as well as understanding the influencing factors to the evolution of the harmonics. The results, aggregated in a magnetic model called FiDeL (Field Description for the LHC) [3], allow to predict the required corrector settings along the LHC cycle in order to compensate field errors.

To achieve the target 16 T in the dipoles for the FCC-hh and the HE-LHC, a change of the superconductor from the NbTi, which was used in the LHC dipoles, to Nb_3Sn is necessary. This superconductor features a larger filament size, which leads to a different persistent current contribution [4, 5], which is a major contribution to the field quality of the 16 T dipoles. In the case of the HE-LHC, where the option of injecting from the current Super Proton Synchrotron (SPS) at CERN with an injection energy of 450 GeV is considered, the large foreseen energy swing leads to another increase of the persistent current contribution at low field. To reduce this effect, measures were taken such as the reduction of the filament size from 50 µm to 20 µm and the inclusion of artificial pinning centers to reduce the magnetization at low fields. For the LHC dipoles, where NbTi is used, the filament size

is around 7 µm [6]. The field quality tables for the 16 T dipoles, showing both the systematic and persistent current contributions, are presented in [7].

Due to this large sextupole component of e.g. 50 units (at a reference radius of 17 mm) at 450 GeV [7] in the HE-LHC, a similar systematic setting error of the MCS of 10 %, as was assumed for the LHC [8], would result in a drastically more challenging situation. For comparison, in the LHC a systematic b_3 between 4.5 to 5.7 units (with one notable exception being arc 78 with 2.5 units) is corrected for [9]. MCS setting errors could potentially occur due to a limited magnetic measurement accuracy, imperfect models of the dynamic contributions as well as from a rapid change in the order of a few seconds [10] coming from the snap-back. Again, while the first order chromaticity generated from this uncorrected sextupole component is easily corrected, for the other effects such as amplitude detuning the identification of the contribution in the presence of other multipoles and subsequent correction might prove significantly more difficult. This temporary situation of a large local b_3 could represent the overall limitation for the DA during the cycle, and as such possibly the overall collider performance.

A large systematic b_3 was studied in the LHC during this MD. Due to the better field quality of the LHC dipoles in comparison to what is expected for the 16 T Nb_3Sn dipoles, the MCS are used to mimic a large systematic b_3 in the dipoles. The chromaticity was then corrected using the main sextupoles (MS). Following the change in the spool piece corrector powering, the dynamic aperture was measured and results are presented in this report.

The change of powering of the MCS also allows to study possible changes in the linear optics and coupling due to misalignments of the sextupole spool piece correctors.

2 Measurement summary

In Tab. 1 the key parameter of MD3603 are summarised.

Table 1: Summary of the MD parameters.

MD # :	3603
FILL # :	6971
Beam Process:	RAMP_PELP-SQUEEZE-6.5TeV-ATS-1m-2018_V3_V1_HeatLoad@0_[START]
Date:	24/07/2018
Start Time:	09:00
End Time:	16:15
Beam :	LHCB1
Note:	MD3623 in parallel in Beam 2

2.1 Procedure

The time-line of the MD is presented in Tab. 2. In parallel, MD3623 took place in Beam 2. While mostly independent, certain activities such as the chromaticity measurements had

Table 2: Time-line of the MD.

9:00	Start of the MD
10:45 → 11:45	Turning off MCS spool pieces arc by arc, correcting chromaticity after each arc depowering using the main sextupoles (MS)
11:16 → 11:37	During the depowering AC-Dipole kicks were conducted
12:00	Issues with bunch profile requiring TL steering
12:07 → 12:20	Optics measurement with AC-Dipole
13:00 → 13:45	Setting MCS spool pieces to twice nominal strength with opposite sign and correction of chromaticity with main sextupoles
13:45 → 14:05	Measurement of horizontal amplitude detuning
13:57 → 14:00	Optics measurement with AC-dipole excitation and RF-modulation
14:07 → 14:25	Measurement of vertical amplitude detuning
14:40 → 16:15	DA Measurement with the aperture kicker
16:15	End of MD 3603

to be coordinated as they affected both beams. The MD was performed at the injection energy of 450 GeV using one pilot bunch (with a beam intensity $\approx 5 \cdot 10^9$ p^+) and the nominal injection optics. The fractional tunes were set to 0.28/0.31 and chromaticity was corrected to $Q'_{x,y} = 3$ units. Upon the start of the MD, collimators including the injection protection were retracted to coarse settings to provide ample aperture for AC-dipole and aperture kicker (MKA) excitation. Before the change of powering, the initial coupling was assessed, and a coupling correction was deemed not necessary (residual coupling equivalent to coupling knob settings [11] of $C^- = -2.3 \cdot 10^{-3} - 1.3i \cdot 10^{-3}$ in an ideal machine). Starting with Arc12, the current for the MCS was set to 0 arc by arc, as illustrated in Fig. 1.

After each sector depowering, the chromaticity was corrected using the arc sextupoles. Due to issues with the beam quality traced backed to injection oscillations, transfer line steering was carried out at this point. Additionally, linear optics measurements using the AC-dipole were conducted after the depowering of all MCS. In the following, the MCS currents were set to twice the nominal strength but with opposite polarity. After each change in the circuit powering, the chromaticity was corrected with the MS. Linear optics measurement were performed to assess the impact of a possible misalignment of the MCS on coupling and beta-beating. These were followed by single plane AC-dipole excitation to assess amplitude detuning and also for potential assessment of forced dynamic aperture. Lastly, large amplitude excitation with the aperture kicker (MKA) were performed to assess the free dynamic aperture. Before each MKA kick, the previous pilot bunch was dumped and a new bunch was injected. The kick strength of the MKA was limited to 7 $\sigma_{nominal}$ and 9.5 $\sigma_{nominal}$ in the horizontal and vertical planes, respectively, where $\sigma_{nominal}$ refers to the beam size using the LHC design normalized emittance of ϵ_n =3.75 µm.

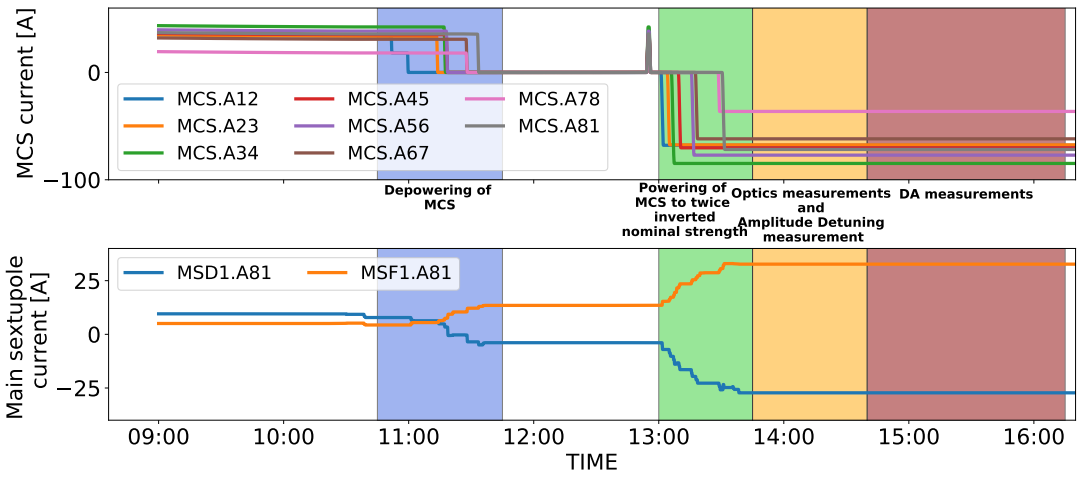

Figure 1: Evolution the current from the power supplies of the sextupole spool piece (MCS) correctors (top) and of the arc sextupole, grouped into sextupoles close to the focussing (MSF) and defocussing quadrupoles (MSD) (bottom). Here, only the current for the MS in Arc81 is displayed. The MS in the other arcs were powered with the same current.

2.2 Results

As the optics at the beginning of the MD is the nominal injection optics, which has already been thoroughly analysed during the LHC commissioning phase, no in-depth optics measurements were conducted at this point. A comparison between the beta-beating obtained from a single kick at the beginning of the MD to the beta-beating assessed during the LHC optics commissioning in April 2018 is presented in Fig. 2. As expected, no significant difference is

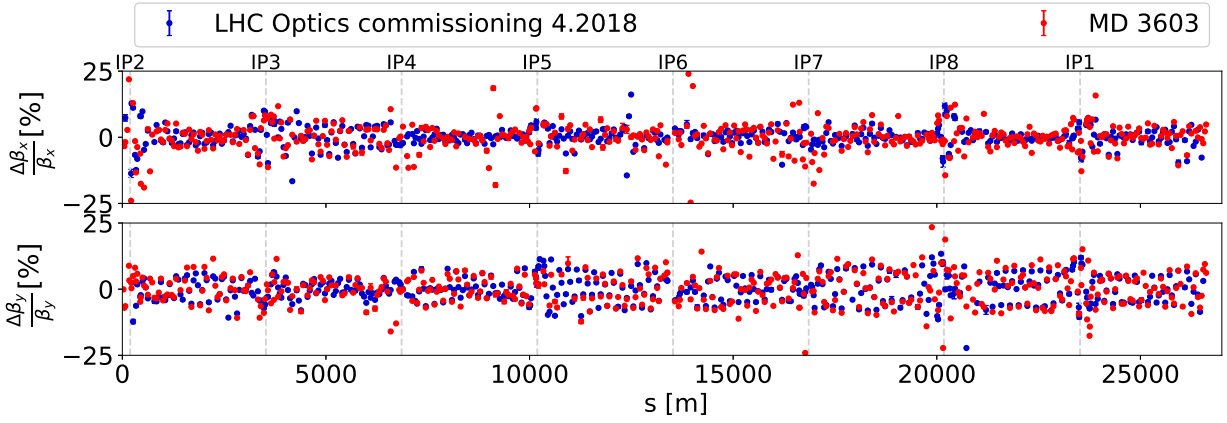

Figure 2: Comparison between beta-beating measured for injection optics during the LHC optics commissioning in April 2018 and in the beginning of the MD.

observed. As for coupling, a small difference in the amplitude is observed, shown in Fig. 3. During the MD the fractional tunes were set to 0.28/0.31, whereas during commissioning the injection tunes 0.275/0.295 were used. No notable difference in the coupling structure is observed. Assuming that coupling sources have remained the same between commission-

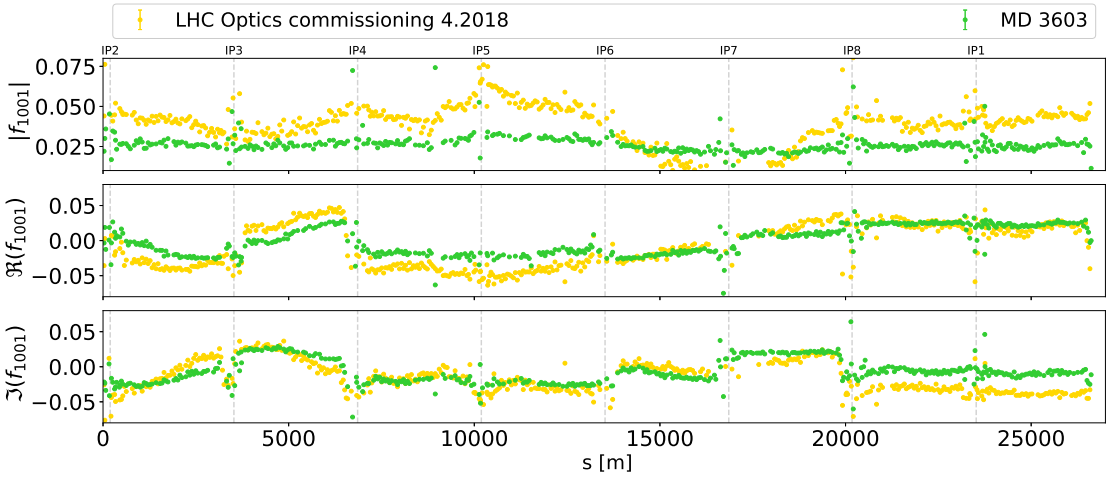

Figure 3: Comparison between difference coupling resonance driving term measured for injection optics during the LHC optics commissioning in April 2018 and in the beginning of the MD.

ing and MD and neglecting the slight change of the β-functions, this change of the tunes leads to a change of the resonance driving term (RDT) amplitude of the difference resonance ($Q_x - Q_y = p$) between commissioning and the MD settings of about a factor

$$\left| \frac{1 - e^{2\pi i (Q_x^{MD} - Q_y^{MD})}}{1 - e^{2\pi i (Q_x^{commissioning} - Q_y^{commissioning})}} \right| \approx 1.5 \ . \tag{1}$$

Single AC-dipole excitations were performed after some arc depowering steps to assess the change in coupling. One example is presented in Fig. 4 for the case of Arc12. A drastic

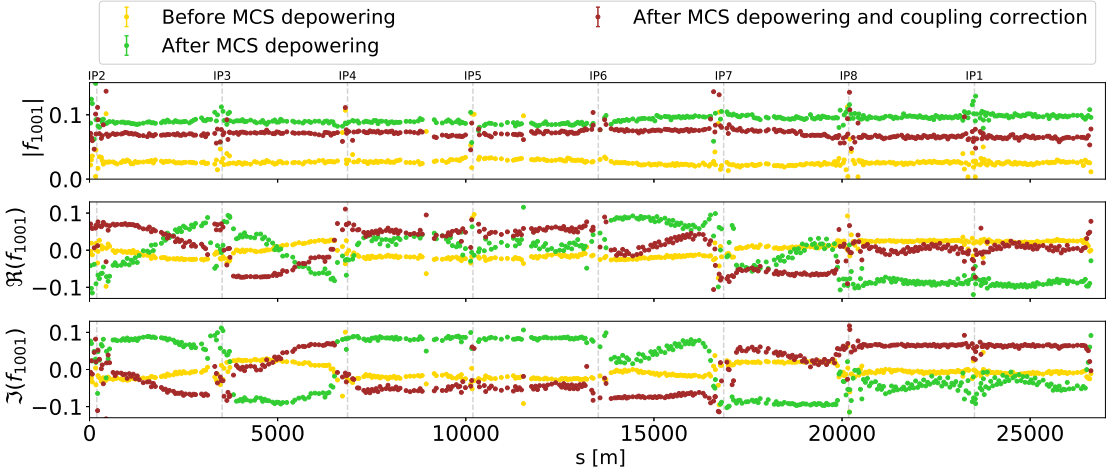

Figure 4: Change in Coupling after depowering the MCS in Arc12.

increase of about a factor 2 is observed in $|f_{1001}|$ before any coupling corrections were applied, highlighting the contribution of the MCS to the coupling in the LHC [12]. After reaching the final MCS powering and the subsequent chromaticity correction with the main sextupoles

linear optics measurements were conducted, which are presented in Fig. 5 together with the beta-beating for the nominal MCS powering. In the mispowered MCS configuration

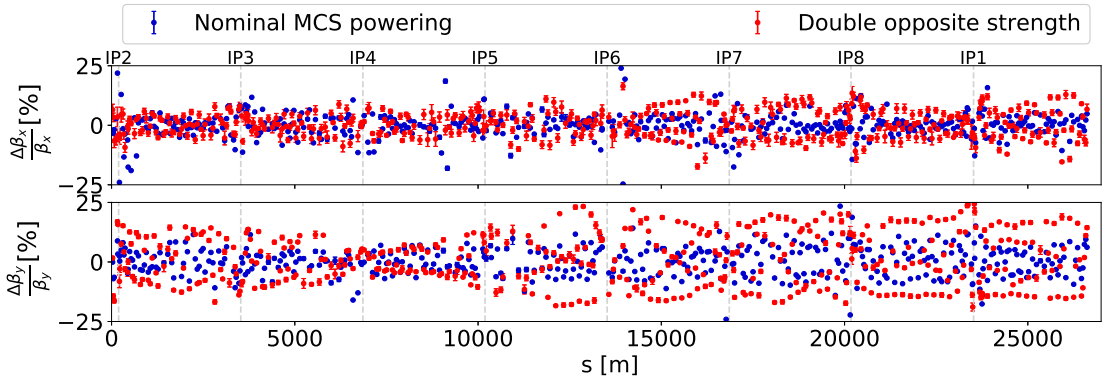

Figure 5: Comparison of beta-beating between the nominal MCS setting and powered with twice the strength and opposite sign.

a significantly higher beta-beating than in the nominal case is observed, especially in the vertical plane where a maximum beta-beating of 25% is obtained. The change in the linear optics can mostly be attributed to feed-down via horizontal misalignment of the sextupole spool pieces or main sextupoles. Similarly, a change in the coupling structure between the two MCS powering cases, as presented in Fig. 6, can be noted. However, the overall

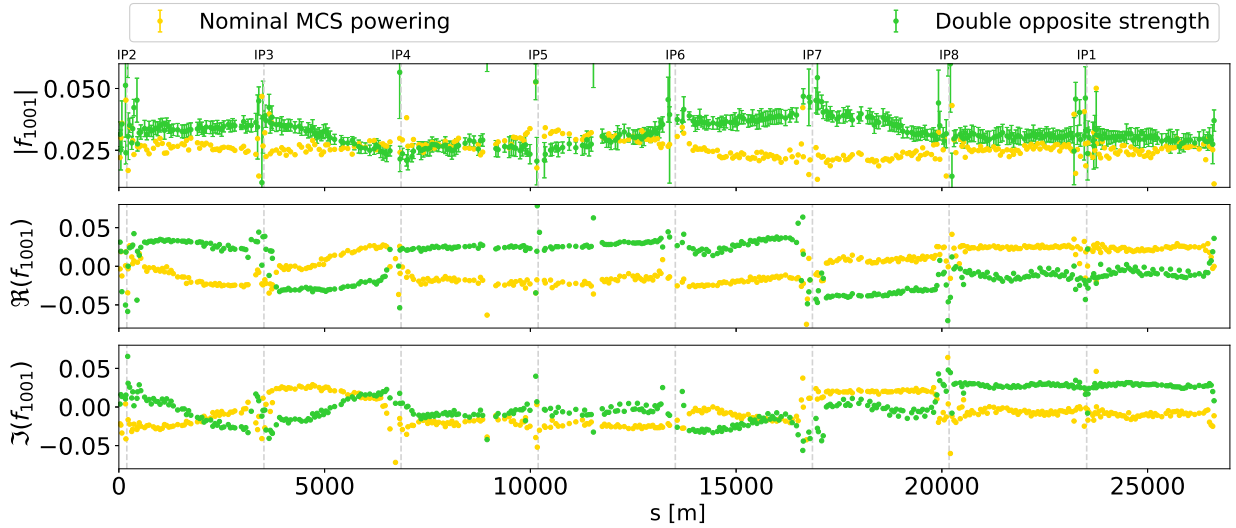

Figure 6: Comparison of coupling between the nominal MCS setting and powered with twice the strength and opposite sign.

coupling is similar between the two cases and no special correction was considered necessary. Presented in Fig. 7 and Fig. 8, no drastic change in the closed orbit is observed.

The amplitude detuning measurements were analysed following the same algorithm as described in [13]. During the measurements, a tune drift was observed, for which the measurements were corrected for. In Fig. 9, the horizontal and vertical tunes, measured by the

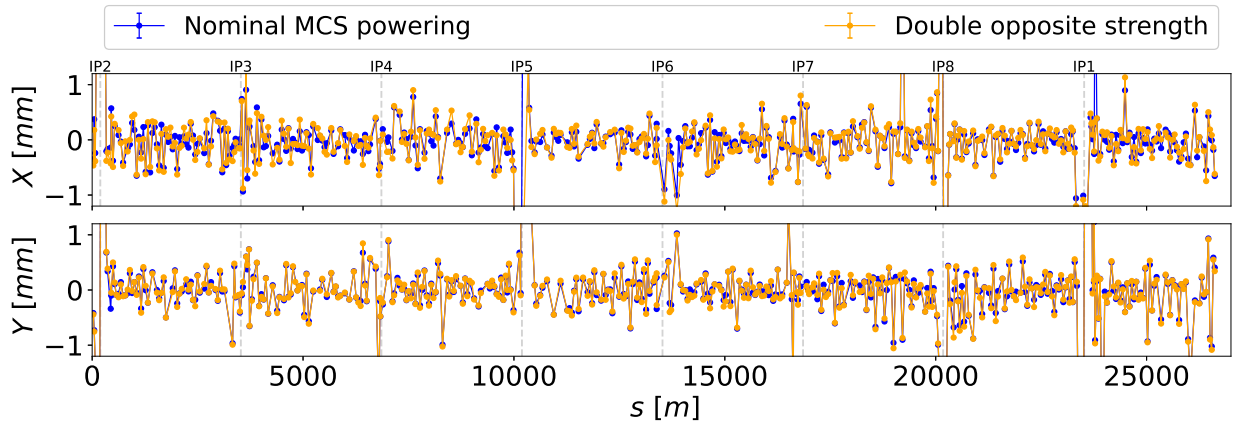

Figure 7: Comparison of closed orbit between the nominal MCS setting and powered with twice the strength and opposite sign.

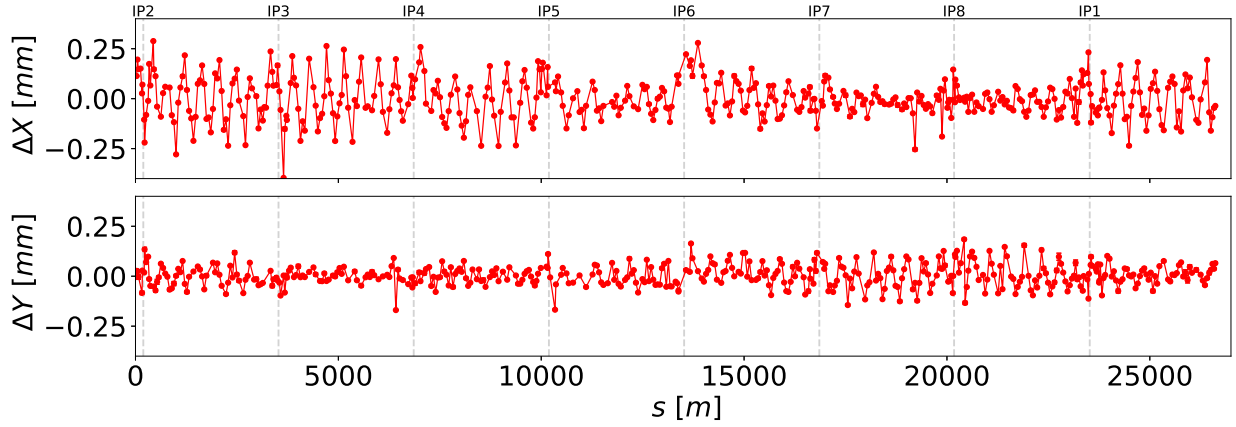

Figure 8: Difference between the closed orbit of the nominal MCS setting and when powered with twice the strength and opposite sign.

BBQ [14], during the horizontal excitations are presented, showing a tune drift of roughly 10^{-3} over a time span of 20 minutes. The results of the amplitude detuning measurements are presented in Fig. 10.

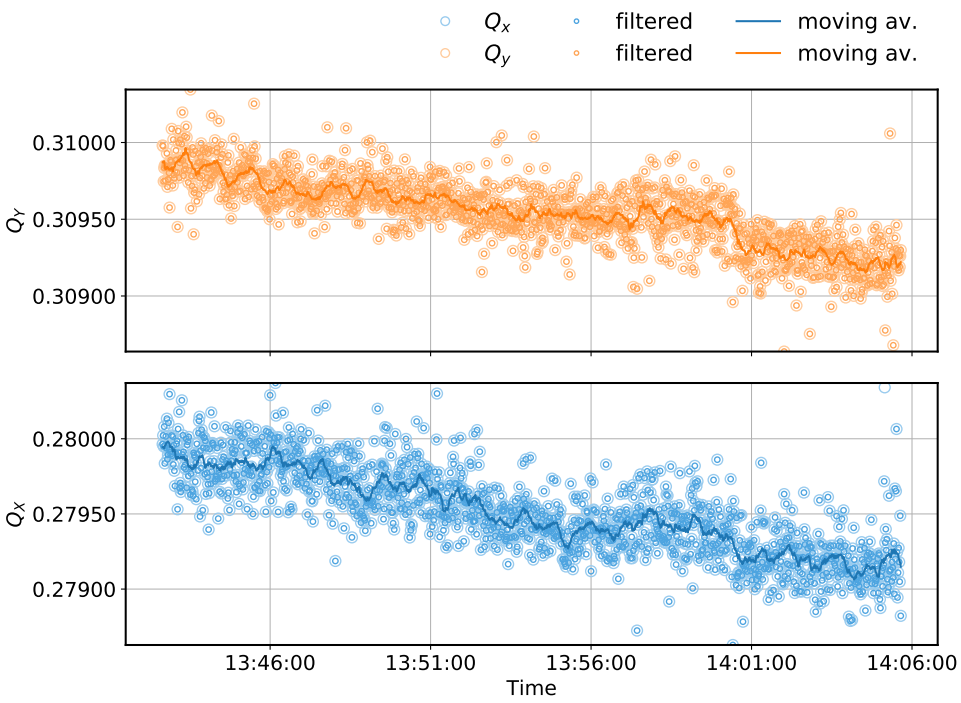

Figure 9: BBQ tune measurement during AC-Dipole excitations in the horizontal plane.

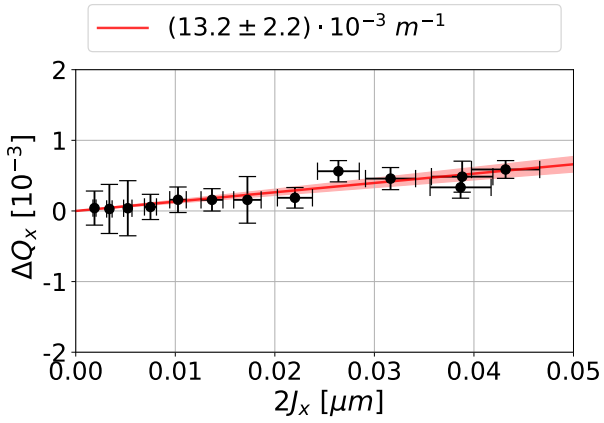

(a) $\delta Q_x/\delta 2J_x$

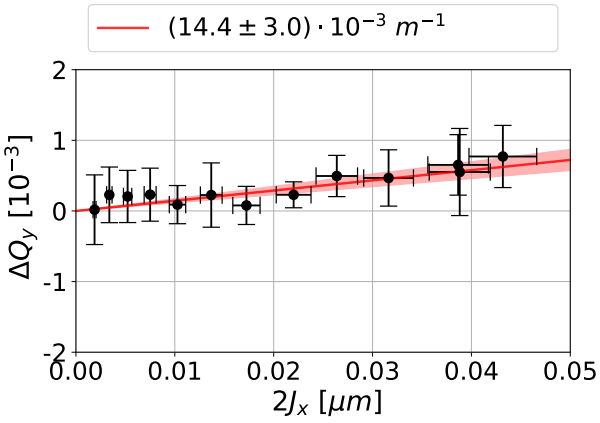

(b) $\delta Q_y/\delta 2J_x$

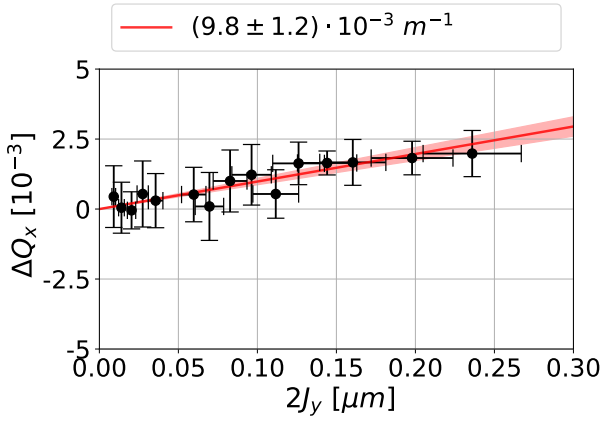

(c) $\delta Q_x/\delta 2J_y$

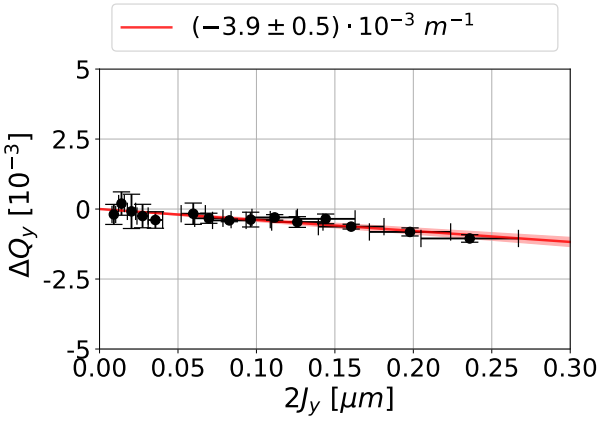

(d) $\delta Q_y/\delta 2J_y$

Figure 10: Measured amplitude detuning during MD3603 for the targeted MCS powering. Note that here the direct amplitude detuning is factor 2 larger compared to the case of free excitations due to the use of the AC-Dipole [15].

In Fig. 11, the spectrum at the BPM.10L1.B1 is presented during one vertical AC-dipole excitation. In both planes, spectral lines corresponding to decapolar resonances are

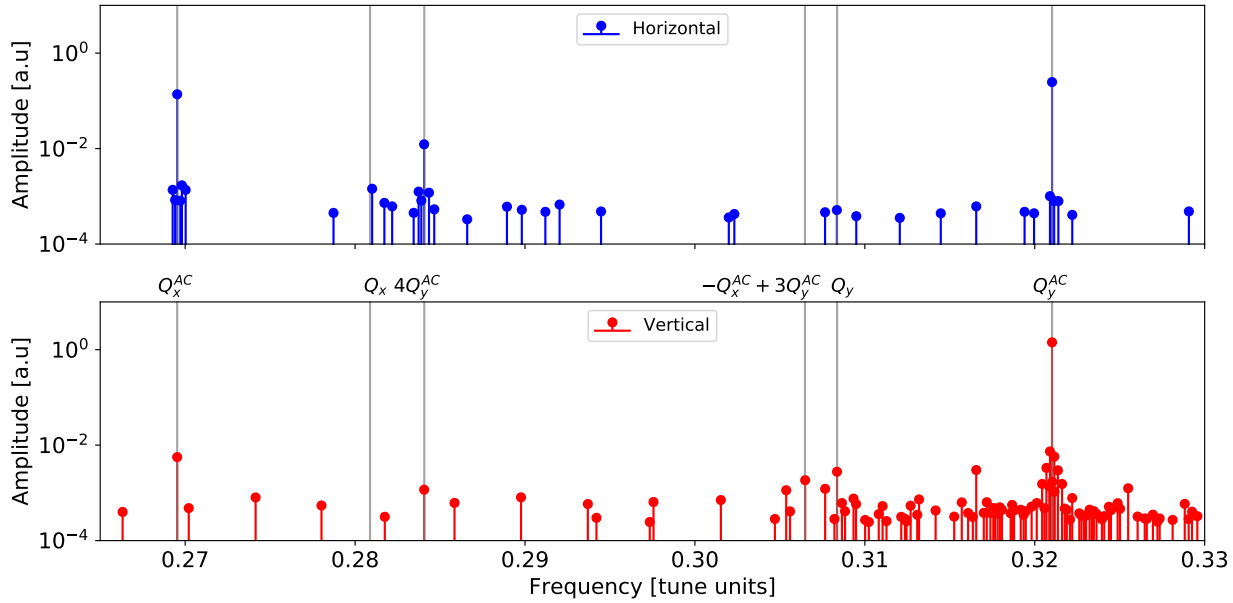

Figure 11: Horizontal and vertical spectrum of BPM.10L1.B1 for one AC-Dipole excitation.

found close to the natural tunes. In the horizontal plane, the $4Q_y^{AC}$ spectral line, where $Q_y^{AC} = Q_y + 0.012$ is the driven tune of the AC-Dipole, is found close to the natural tune Q_x. The driven tune in the horizontal plane is $Q_x^{AC} = Q_x - 0.01$. For the vertical case, Q_y is in the vicinity of the $-Q_x^{AC} + 3Q_y^{AC}$ spectral line. However, these do not disturb the amplitude detuning measurements as the resolution of the frequency analysis is sufficient to distinguish between the lines. Strong decapolar lines, disturbing amplitude detuning measurements have already been reported in [13], although at a beam energy of 6.5 TeV.

During the vertical kicks, increasing losses are visible in the intensity, measured by the fast beam current transformer (FBCT) [6] and displayed in Fig. 12. Such losses were not seen in the preceding horizontal kicks, where the highest amplitude kicks were more than a factor 2 smaller than the largest vertical excitations.

Given the kick amplitude below $6\sigma_{nominal}$ and the fully retracted collimators, these losses during the vertical excitations with the AC-dipole are attributed to particles crossing the boundary of stable motion, called forced dynamic aperture [16]. In a simplified one dimensional model the forced dynamic aperture relates to the intensity losses via

$$DA^{forced} = J_z^{forced} - \epsilon_z \ln \frac{\Delta I}{I}, \tag{2}$$

where $\frac{\Delta I}{I}$ is the relative intensity loss, z the excitation plane, J_z^{forced} the action of the excitation and ϵ_z the emittance of the bunch.

The emittance in between the kicks was logged using the BSRT and beforehand a reference measurement using the wire scanner (BWS) was performed. Horizontal and vertical normalized emittance during the amplitude detuning measurements are displayed in Fig. 13.

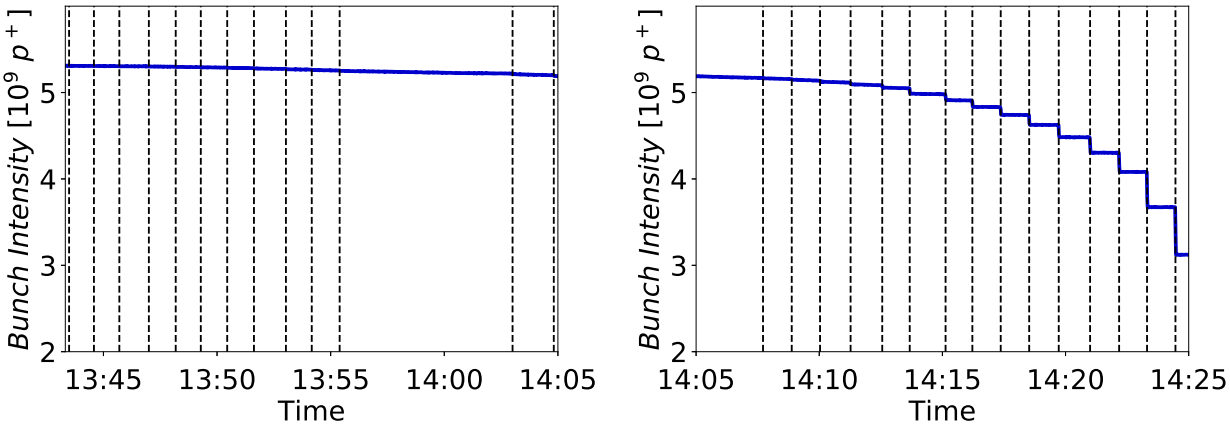

(a) Intensity during horizontal excitations (b) Intensity during vertical excitations

Figure 12: Losses in the beam intensity during AC-dipole excitations.

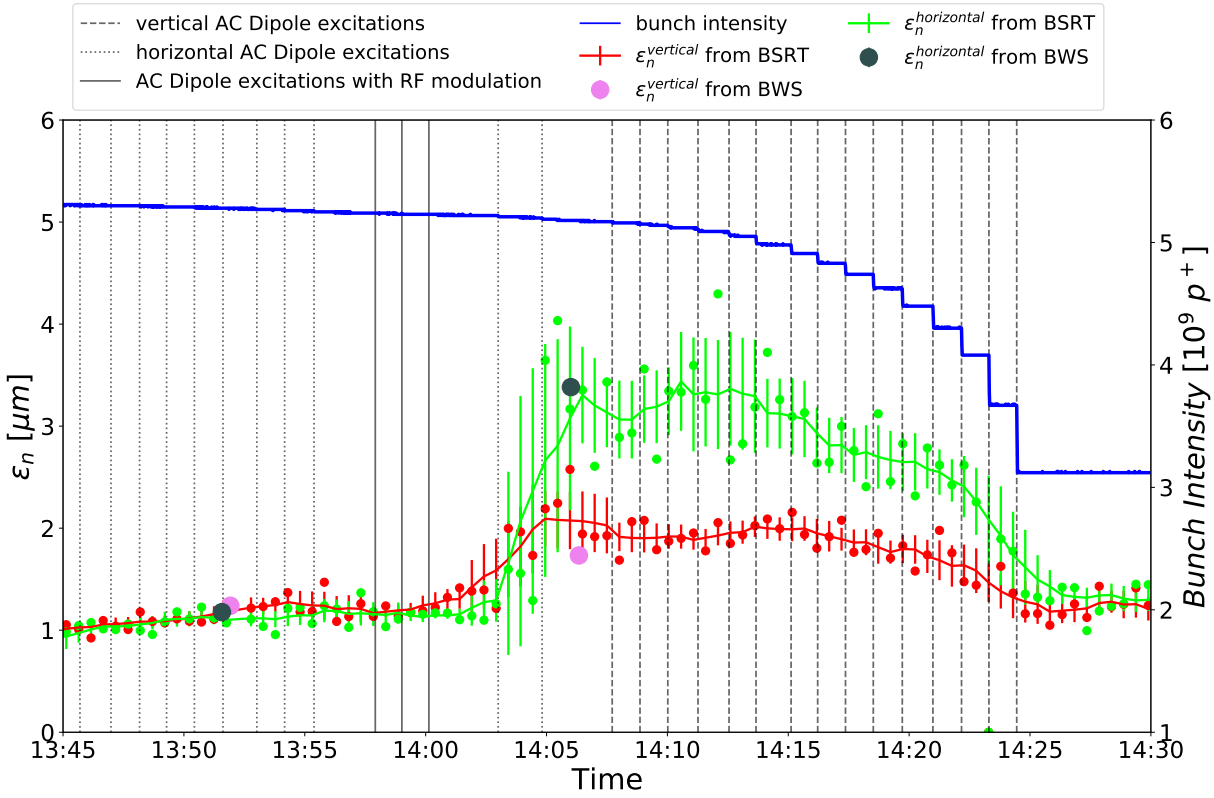

Figure 13: Measured normalized emittance as measured by the BSRT and the BWS during the AC-dipole excitations and the beam intensity from the FBCT. The kick times are displayed as vertical dashed lines.

The emittance measured with the BWS beforehand agrees well with the BSRT measurements and no correction has been applied to the BSRT measurements. For the calculation of the forced DA, a moving average of the measured BSRT emittance was performed using the current value and three measurements before and after the current timestamp. Beforehand,

sudden drops of emittance were removed from the dataset, these being assumed to be false readings caused by the AC-dipole excitation. Notably, the emittance in both planes increases drastically during the two last horizontal AC-dipole excitations. This is observed in both BSRT and BWS measurements. Following the vertical kicks, a decrease of the normalized emittance of about a factor 3 in the horizontal plane and about factor 2 in the vertical plane is observed. In Fig. 14, the projection of the image captured by the BSRT to the horizontal and vertical planes is displayed, together with mean and standard deviation of the fitted Gaussian profile, indicated by white lines. At around 14:04, a sudden dip of the

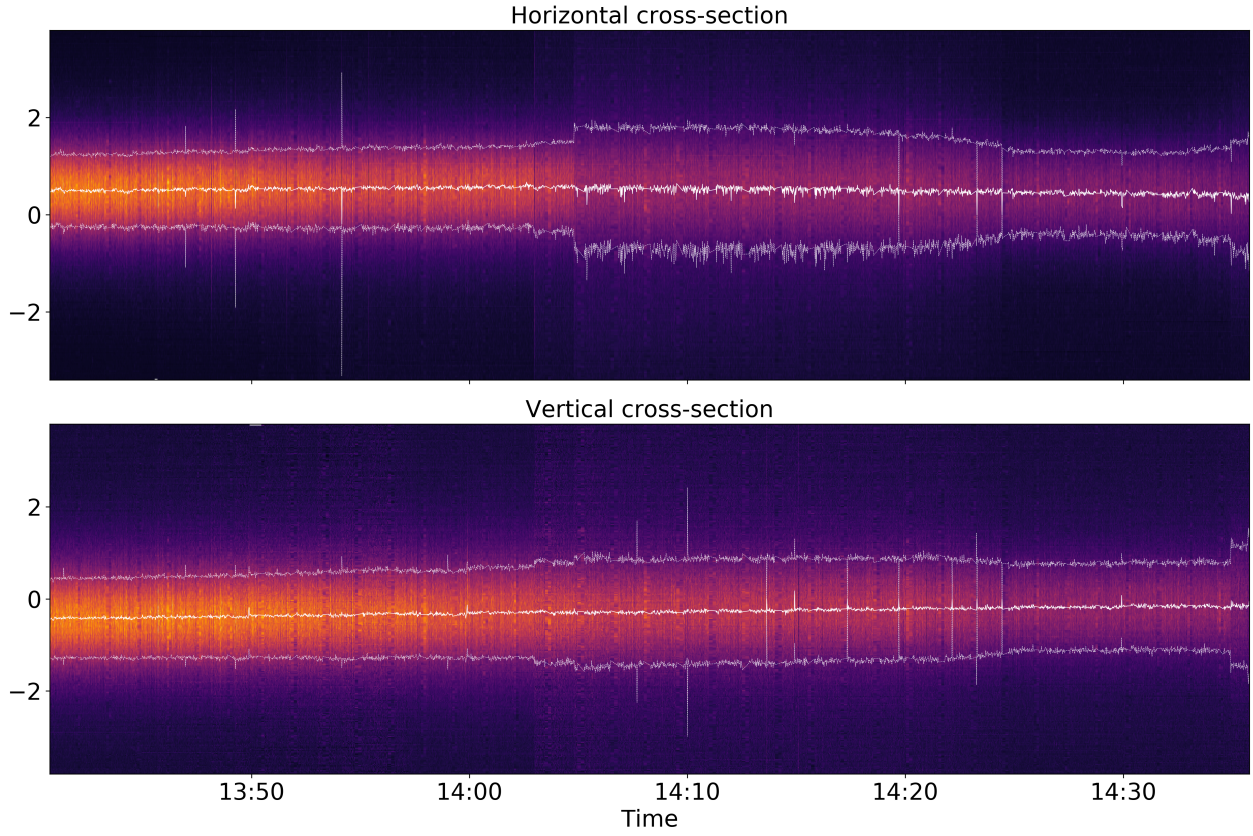

Figure 14: Logged cross-section from BSRT.

peak signal is observed, together with a sudden increase of the standard deviation, more visible in the horizontal plane. In Fig. 15, the measured density and the fitted Gaussian profile are displayed before the emittance blowup, during the vertical AC-dipole excitations and afterwards.

From Fig. 15b top, the increase of the spotsize in the horizontal plane is observed together with an overpopulation of the tails. The subsequent decrease of the horizontal spotsize may stem from particles with large horizontal action being lost due to an excitation, either through coupling with the vertical plane, due to a small excitation provided by the AC-dipole also in the horizontal plane to allow for measuring the crossplane amplitude detuning, as is already described in [17], or, given the positive measured cross plane amplitude detuning and thus particles with large horizontal action being closer to the driven vertical tune Q_y^{AC},

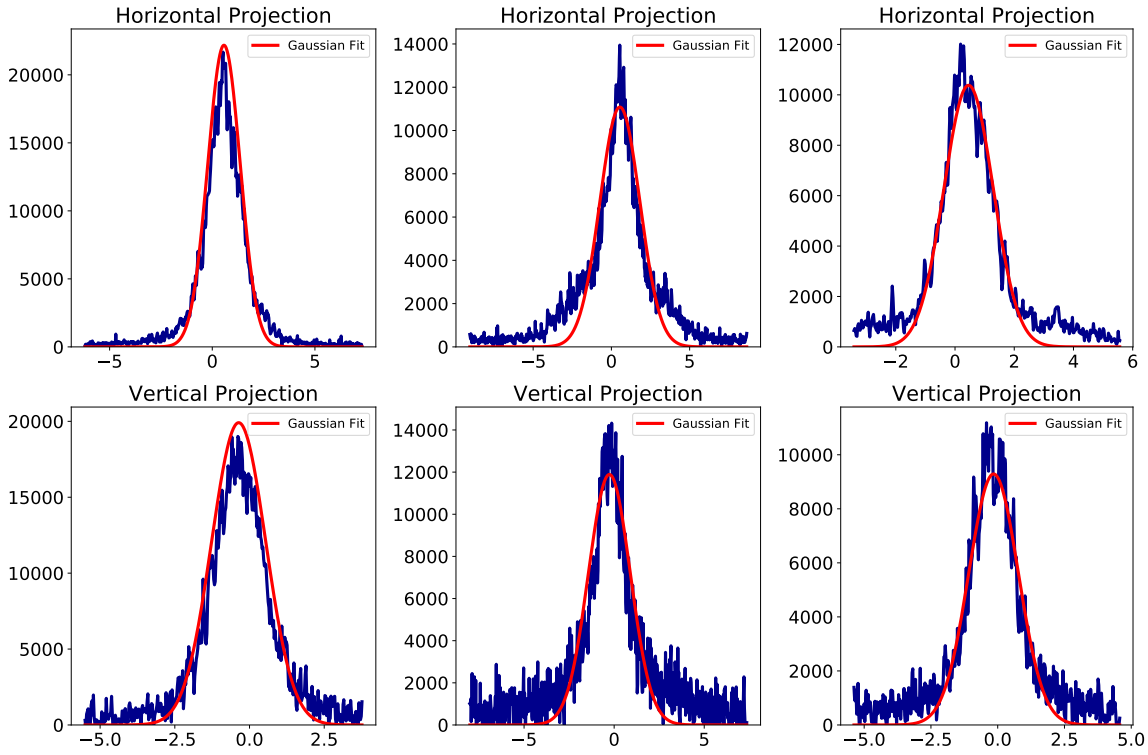

(a) Logged cross-section at 13:50

(b) Logged cross-section at 14:09

(c) Logged cross-section at 14:30

Figure 15: Projections of the logged BSRT signal to the horizontal and vertical plane.

receiving a stronger kick from the AC-Dipole and subsequently being lost. As the readings in vertical plane appear to have been less distorted by this effect, no correction to the measured emittance in the vertical plane was applied. The unwanted beam blow-up went unnoticed during the MD and as such, no corrective measures such as reinjecting a new pilot bunch were taken. In Fig. 16 the relative losses of the beam intensity are shown. Unfortunately, the overpopulation of tails in the horizontal plane and loss of these particle with large horizontal action spoil the measurement of the vertical forced dynamic aperture. Given the significant contribution to the beam losses from the horizontal large amplitude particles, from the given data is not possible to extract just the beam loss of particles with large vertical amplitude and as such no vertical forced dynamic aperture fitting the observed beam loss could be found, showing a clear point to watch for in future forced DA measurements. Using the last point as reference, it can however be stated that the forced dynamic aperture is above $5.61 \pm 0.35\ \sigma_{nominal}$, assuming a nominal normalized emittance of 3.75 µm. Due to occurrence of additional resonances as well as an increase of the amplitude detuning during forced oscillations [15], the forced DA is in general smaller than the free dynamic aperture [16].

Following the AC-dipole kicks, the free dynamic aperture was measured using the MKA[1]. After each excitation, the beam was dumped and a new beam was injected. The beam losses

[1]As was already reported in [18], the horizontal and vertical kicker are swapped with respect to what is set in the software.

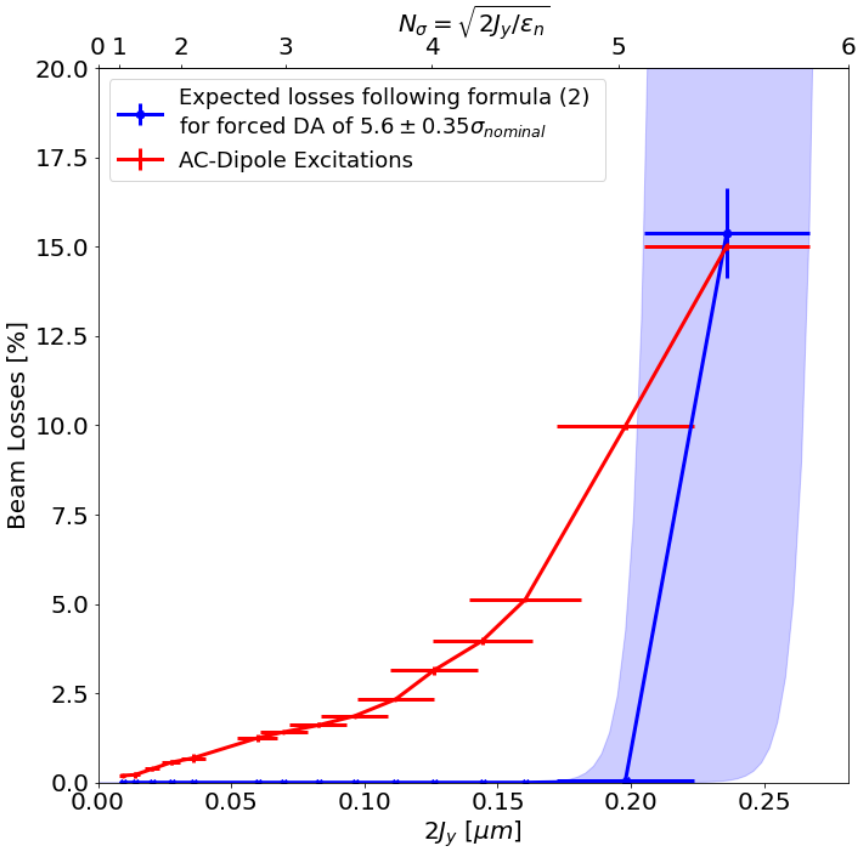

Figure 16: Measured losses of beam intensity during vertical AC-dipole excitation together with expected losses following formula (2).

were calculated using the intensity from the FBCT before the excitation and 11 s after the excitation. The kick amplitudes and the associated beam intensity losses are shown in Fig. 17.

Here, significant losses can only be seen for diagonal excitations above a kick-amplitude of 9 $\sigma_{nominal}$. For horizontal excitations no losses are observed even at the maximum amplitude the MKA could provide during the MD. Assuming an uncertainty of 1% on the losses measured with the BCT for the largest horizontal excitation with a kick amplitude of N_σ together with [17]

$$\frac{DA - N_\sigma}{\sqrt{2}} = \mathrm{erf}^{-1}\left[1 - 2\frac{\Delta I}{I}\right] \tag{3}$$

would put the DA in this plane above 9.8 $\sigma_{nominal}$. Due to time constraints, no single kick excitations in the vertical plane were conducted. Using the data obtained from the diagonal excitations the free DA can be calculated following the same procedure as in [19]. Two datasets of kicks were used, one using kick angles between 40° and 50° and another one between 47° and 63°. The measured losses for these kicks are presented in Fig. 18.

For both datasets, the free DA obtained via fitting gives results above 10 $\sigma_{nominal}$.

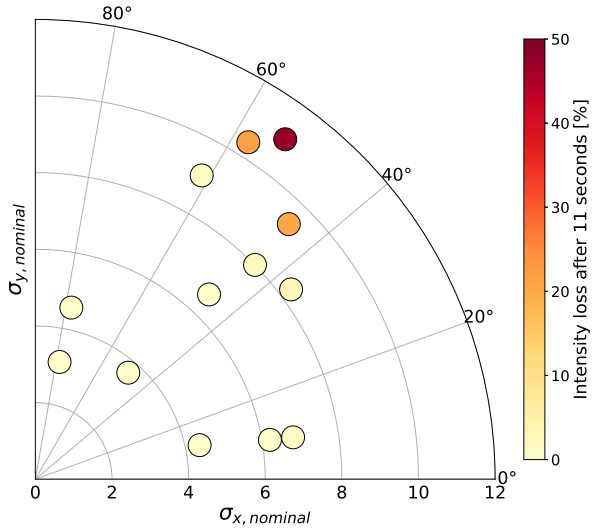

Figure 17: Excitations with the MKA and corresponding intensity losses from the FBCT.

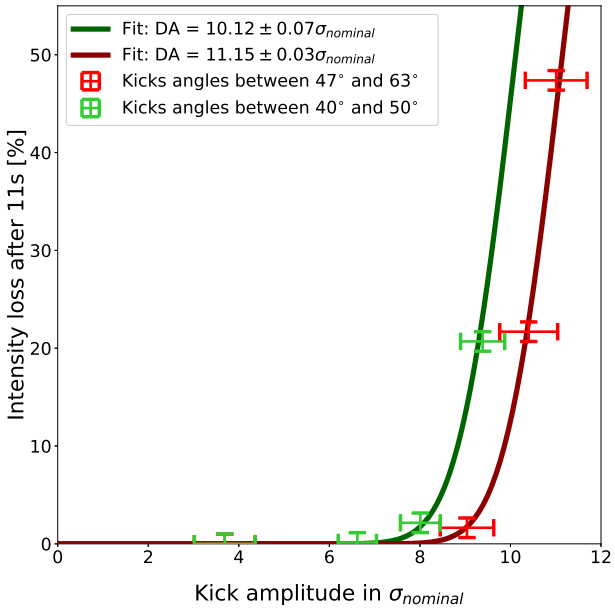

Figure 18: Measured beam intensity losses during the diagonal excitations and fit for obtaining free DA.

3 Comparison to simulation

Tracking studies using the tracking code SixTrack [20] were performed to provide an estimate for the DA expected during the MD. The nominal injection optics as used during the MD is used in the model, with both Landau octupoles and octupole spool pieces depowered as was also the case during the MD. Tunes were set to 0.28/0.31 and the chromaticity was corrected to +3 units using the MS, following the same procedure as used in the MD. For the errors in the magnets, 60 WISE [21] seeds were used, excluding linear errors such as coupling

and β-beating. In the model, the sextupole spool piece correctors and decapole spool piece corrector circuits were used to correct for the average sextupole and decapole field errors of the dipoles in each arc. Particles were tracked for 10^5 turns, equivalent to 11 s in the LHC, and using 5 angles in x-y-space. Due to the exclusion of linear errors in the magnets as well as no misalignments, these simulations were considered optimistic. The resulting DA from these tracking studies with the double inverted MCS powering is compared to the case with the MCS powered with the nominal settings in Fig. 19.

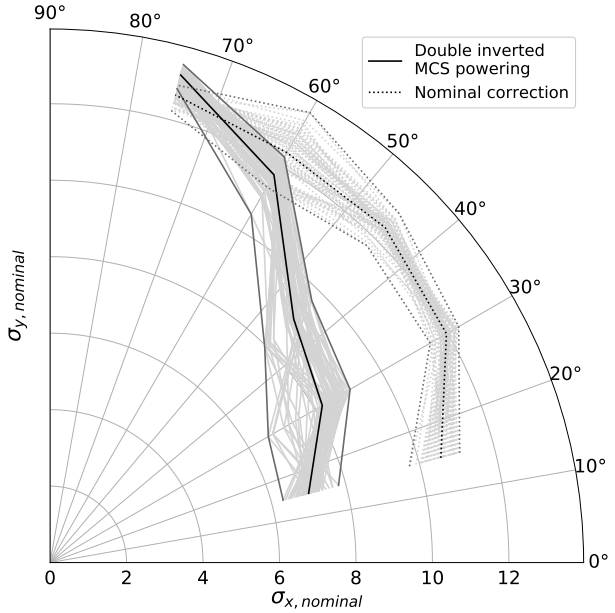

Figure 19: Dynamic Aperture from tracking studies with 10^5 turns using the WISE model with MCS and MS powered as in the MD and with nominal powering.

A clear reduction in the horizontal plane is observed of about 4 $\sigma_{nominal}$. For horizontal excitations, a dynamic aperture below 6 $\sigma_{nominal}$ to 8 $\sigma_{nominal}$ was expected, whereas during the MD the horizontal excitations, no significant losses even at 7 $\sigma_{nominal}$ kick amplitude were observed. With the estimated DA in the vertical plane being above 12 $\sigma_{nominal}$, no dedicated free DA measurements were conducted during the MD as it would lie significantly above the maximum possible kick amplitude. For diagonal excitations, the measured DA of ≥ 10 $\sigma_{nominal}$ tends to be on the upper bound of the tracking studies results. As such, even the simple model, expected to provide an optimistic estimate, seems to rather underestimate the DA in the LHC. Comparing the results from the amplitude detuning measurements to the amplitude detuning in the models, calculated using PTC, shows a significant discrepancy in the vertical detuning term. The comparison for all terms is presented in Fig. 20.

As the Landau octupoles are depowered in the model, three major sources of amplitude detuning detuning remain. The first contribution comes from the uncorrected octupole errors from the dipoles, which are already taken into account by the WISE model. The second contribution is from feed-down of the decapole spool piece correctors, due to misalignment or orbit excursions. From non-linear chromaticity studies, presented in [22], it was concluded that in the LHC a systematic horizontal misalignment of the decapole spool piece correctors (MCD) of about 0.2 mm should be taken into account. The last potential contribution,

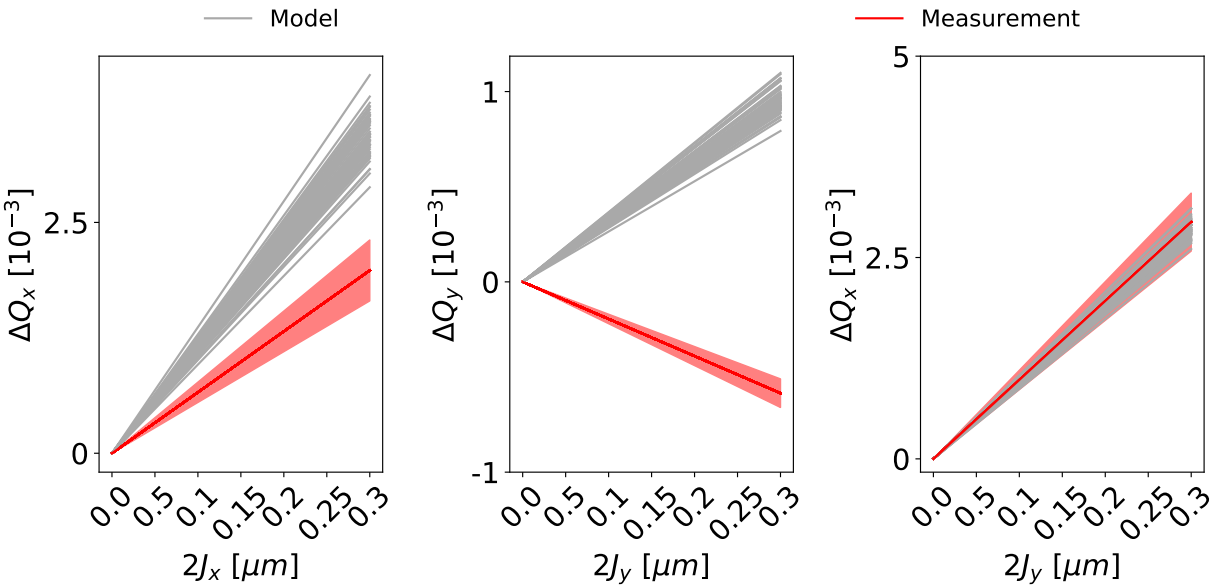

Figure 20: Comparison between the measured amplitude detuning and the amplitude detuning for the WISE seeds.

particularly relevant for this MD, is the second order contribution from the sextupoles to amplitude detuning. While the first two options with its measurement uncertainties are easily implemented in the model, in the third option care has to be taken to properly adjust the phase advances between the sextupole sources to allow for comparing the model amplitude detuning and measured one. In these simulations, the amplitude detuning coming from the uncorrected dipole octupole errors and the misalignment of the MCD were shown to be negligible compared to the contribution from the sextupoles. As a simple study to evaluate the impact on the DA from the change in amplitude detuning without adjusting phase advance between sextupoles, the Landau octupoles were used instead to match the amplitude detuning to the measured values. The tracking results using the updated model together with the DA from measurements are presented in Fig. 21.

Compared to the previous results, an increase of the dynamic aperture in the horizontal plane is noted whereas in the vertical plane and for diagonal excitations a slight decrease of the DA occurs. The measured DA is now in good agreement with the simulations. The amplitude detuning was therefore a key ingredient for particle stability. In Fig. 22, the forced dynamic aperture from single particle tracking simulations is presented using the same model as employed also for the free dynamic aperture studies. Contrary to those studies however, only one realization of the magnetic errors (seed) is used. The AC-Dipole settings were set as was used in the MD. The driven tunes were $Q_x^{ac} = Q_x - 0.01$ in the horizontal and $Q_y^{ac} = Q_y + 0.012$ in the vertical plane. The oscillation amplitude is ramped up over 2000 turns and is kept constant for 6000 turns. The action is then obtained by performing a frequency analysis on the first 200 turns, captured at the beam position monitor $BPM.22L1.B1$, at flattop and scaling the amplitude of the mainline with the β-function. The obtained action is then normalized using the nominal emittance of 3.75 µm. The tracking simulation show a forced DA above 9 $\sigma_{nominal}$ for a pure vertical excitation. Given the aforementioned issues

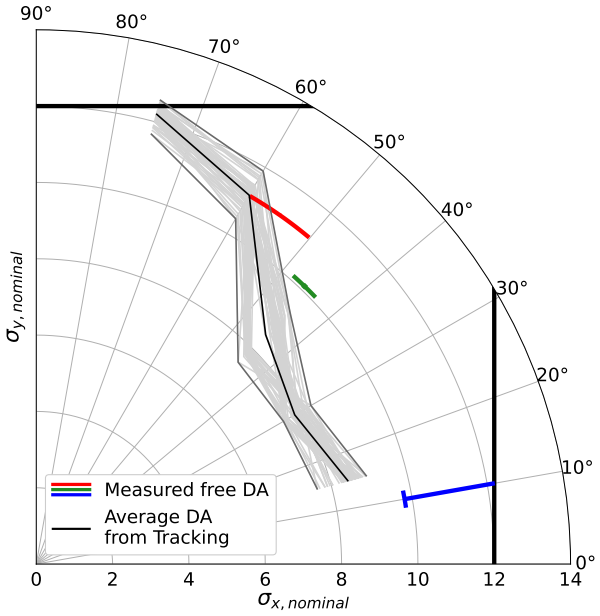

Figure 21: Dynamic Aperture from tracking studies with 10^5 turns using the WISE model and matched amplitude detuning to the measured values together with DA inferred from the measurements. The physical aperture is indicated with black lines.

during the forced dynamic aperture measurements, no conclusion on the validity of the model can be drawn. Using Eq. 2 and the vertical forced DA from the simulations, no loss should have been observed at the maximum kick amplitude of 5.4 $\sigma_{nominal}$.

4 Conclusion

During MD3603, the dynamic aperture in the presence of strong local sextupole fields was successfully assessed. The measurements of free and forced dynamic aperture show a DA above 7 $\sigma_{nominal}$ for horizontal excitations, above 10 $\sigma_{nominal}$ for diagonal excitation and a forced DA above 5.6 $\sigma_{nominal}$ in case of vertical forced excitations. Initial tracking studies using a simple model, thought to provide optimistic estimates, were shown to actually provide lower values than what is measured. One key difference between the simple model and measurement was identified to be the amplitude detuning. Once corrected for in the model, simulation and measurement tend to agree better, showing that the DA in the LHC in the presence of large uncorrected sextupole error is of no concern. In turn, the situation for the HE-LHC or FCC-hh does not seem as severe as initially estimated. As for this case, the amplitude detuning, in part stemming from the strong sextupolar sources, was identified to have the largest impact on DA, a careful assessment of this could allow to find a correction using the octupoles to allow for minimal impact on the operational performance.

5 Acknowledgments

Many thanks go to the operators and EIC who assisted in carrying out the MD.

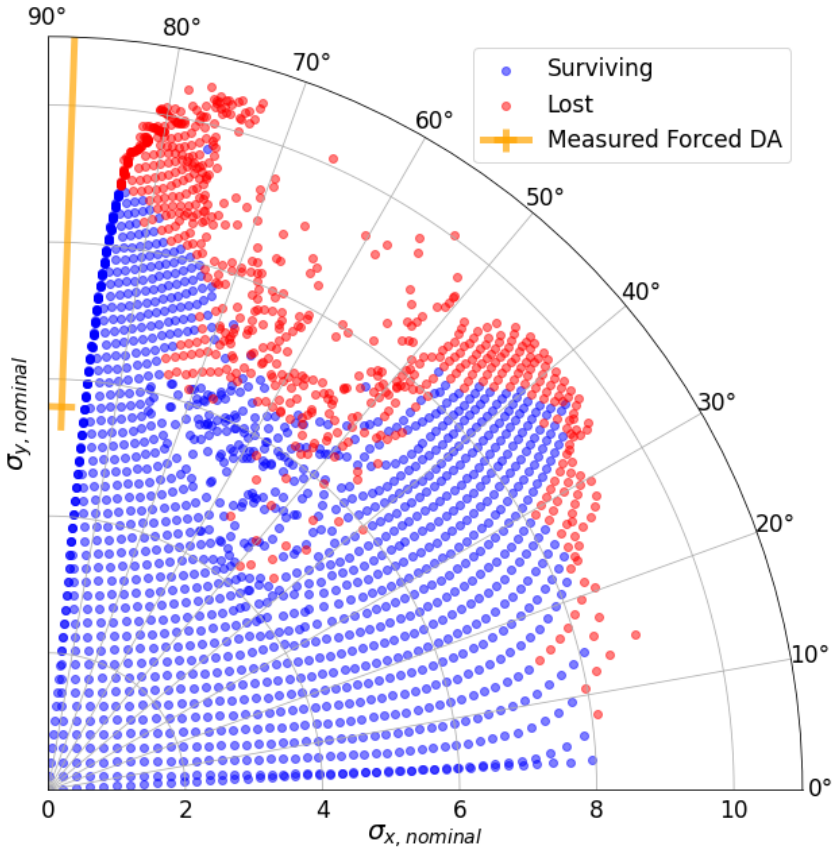

Figure 22: Forced Dynamic Aperture from tracking studies using the WISE model and matched amplitude detuning to the measured values

References

[1] S. Fartoukh. LHC Installation Scenarios and Dynamic Aperture. Technical Report CERN-LHC-Project-Report-449, CERN, Geneva, Dec 2000.

[2] S. Fartoukh. Installation strategy for the main dipoles. In *Proc. 9th European Particle Accelerator Conf. (EPAC'04), Lucerne, Switzerland, Jul. 2004*, pages 176–178, 2004.

[3] N. J. Sammut, J. Micallef, and L. Bottura. *The field description for the Large Hadron Collider*. PhD thesis, 2006. Presented on 12 Oct 2006.

[4] S. Izquierdo Bermudez, L. Bottura, and E. Todesco. Persistent-current magnetization effects in high-field superconducting accelerator magnets. *IEEE Transactions on Applied Superconductivity*, 26(4):1–5, June 2016.

[5] V. V. Kashikhin and A. V. Zlobin. Persistent Current Effect in 15-16 T Nb_3Sn Accelerator Dipoles and its Correction. In *Proceedings, 2nd North American Particle Accelerator Conference (NAPAC2016): Chicago, Illinois, USA, October 9-14, 2016*, page THA1CO04, 2017.

[6] O. S. Brüning, P. Collier, P. Lebrun, S. Myers, R. Ostojic, J. Poole, and P. Proudlock. *LHC Design Report*. CERN Yellow Reports: Monographs. CERN, Geneva, 2004.

[7] S.I. Bermudez and D. Tommasini. Field Quality Table Update for EuroCirCol 16 T design. presented in the 33rd HE-LHC design meeting, https://indico.cern.ch/event/761900/.

[8] O. Brüning and S. Fartoukh. Field Quality Specification for the LHC Main Dipole Magnets. Technical Report LHC-Project-Report-501. CERN-LHC-Project-Report-501, CERN, Geneva, Oct 2001.

[9] P. Hagen, M. Giovannozzi, J.-P. Koutchouk, T. Risselada, F. Schmidt, E. Todesco, and E. Wildner. WISE: A Simulation of the LHC Optics including Magnet Geometrical Data. Technical Report CERN-LHC-PROJECT-Report-1123, Aug 2008.

[10] G. Ambrosio, P. Bauer, L. Bottura, M. Haverkamp, T. Pieloni, S. Sanfilippo, and G. Velev. A scaling law for the snapback in superconducting accelerator magnets. *IEEE Transactions on Applied Superconductivity*, 15(2):1217–1220, June 2005.

[11] R Tomas. Optimizing the global coupling knobs for the LHC. Feb 2012.

[12] T.H.B. Persson et al. LHC optics corrections in Run 2. presented at the 9th LHC Operations Evian Workshop.

[13] Joschua Werner Dilly, Markus Albert, Theodoros Argyropoulos, Felix Simon Carlier, Michael Hofer, Lukas Malina, Ewen Hamish Maclean, Elena Solfaroli Camillocci, and Rogelio Tomas Garcia. Report and Analysis from LHC MD 3311: Amplitude detuning at end-of-squeeze. Mar 2019.

[14] M Gasior and R Jones. The principle and first results of betatron tune measurement by direct diode detection. Technical Report LHC-Project-Report-853. CERN-LHC-Project-Report-853, CERN, Geneva, Aug 2005. revised version submitted on 2005-09-16 09:23:15.

[15] S. White, E. Maclean, and R. Tomás. Direct amplitude detuning measurement with ac dipole. *Phys. Rev. ST Accel. Beams*, 16:071002, Jul 2013.

[16] F. S. Carlier, R. Tomás, E. H. Maclean, and T. H. B. Persson. First experimental demonstration of forced dynamic aperture measurements with lhc ac dipoles. *Phys. Rev. Accel. Beams*, 22:031002, Mar 2019.

[17] E. H. Maclean. *Modelling and correction of the non-linear transverse dynamics of the LHC from beam-based measurements*. PhD thesis, 2014.

[18] E. H. Maclean, F. S. Carlier, M. Giovannozzi, T. H. B. Persson, and R. Tomas Garcia. Report from LHC MD 1399: Effect of linear coupling on nonlinear observables in the LHC. Jan 2017.

[19] E. H. Maclean, R. Tomás, F. Schmidt, and T. H. B. Persson. Measurement of nonlinear observables in the large hadron collider using kicked beams. *Phys. Rev. ST Accel. Beams*, 17:081002, Aug 2014.

[20] SixTrack. http://sixtrack.web.cern.ch/SixTrack/.

[21] P. Hagen, M. Giovannozzi, J.-P. Koutchouk, T. Risselada, S. Sanfilippo, E. Todesco, and E. Wildner. WISE: An Adaptative Simulation of the LHC Optics. (LHC-PROJECT-Report-971. CERN-LHC-Project-Report-971):4 p, Aug 2006.

[22] E. H. Maclean. Optics measurements and misalignment of the b4-b5-spool pieces. presented in the FiDel meeting, https://indico.cern.ch/event/812944/.